IEEE Access
Multidisciplinary ⋮ Rapid Review ⋮ Open Access Journal

Received January 5, 2022, accepted February 9, 2022, date of publication February 11, 2022, date of current version February 22, 2022.

Digital Object Identifier 10.1109/ACCESS.2022.3151066

Space Vector Pulse-Width Modulation Control Strategy for Four-Leg Inverters Under Single Line-to-Ground Faults in Islanded Microgrids

CHANG-GYUN AN[1], BONG-YEON CHOI[2], HOON LEE[1], TAE-GYU KIM[1], KYUNG-MIN KANG[1], MINA KIM[1], YOON-SEONG LEE[1], JUNSIN YI[1], (Senior Member, IEEE), AND CHUNG-YUEN WON[1], (Senior Member, IEEE)

[1]Department of Electrical and Engineering, Sungkyunkwan University, Suwon 16419, South Korea
[2]Mando Corporation, Seongnam 13486, South Korea

Corresponding author: Chung-Yuen Won (woncy@skku.edu)

This work was supported by the Korea Institute of Energy Technology Evaluation and Planning (KETEP) 501 the Ministry of Trade, Industry & Energy (MOTIE) of the Republic of Korea, under Grant 20193810100001B.

ABSTRACT In this paper, we propose a novel switching modulation scheme for three-phase four-leg inverters that enables the separation of the fault points occurring in AC distribution networks. The proposed method is aimed at continuously supplying normal voltage to the remaining healthy phases while applying zero voltage to any faulty phase when a single line-to-ground (SLG) fault occurs in the distribution network. This modulation scheme allows isolation without physically blocking the point of failure. This can prevent unnecessary continuous outages in the AC distribution network. To this end, we propose a novel coordinate transformation method to extract accurate values for the magnitude of unbalanced three-phase voltages. A novel space vector pulse-width modulation (SVPWM) method for switching schemes that are used under fault conditions is also presented. The proposed coordinate transformation considers a plane lying in a three-dimensional (3-D) space that describes the rotation of a three-phase voltage vector. This transformation converts a physical quantity that rotates in 3-D space into a value that moves in two-dimensional (2-D) space. Subsequently, the use of synchronous reference frame (SRF) transformation enables the detection and control of the voltage magnitude in case of an SLG fault. Additionally, switching vectors are selected to apply zero voltage to the faulty phase by analyzing the switching vector diagram of a four-leg inverter. Mathematical analyses conducted for the entire process are detailed herein. Further, the experimental results of four-leg inverters designed for the 10 kW class verify the proposed strategies.

INDEX TERMS Single line-to-ground (SLG), four-leg inverters, three-dimensional (3-D), space vector pulse-width modulation (SVPWM), coordinate transformation, microgrid.

NOMENCLATURE

$X_{a,b,c}$	Variables in a-b-c coordinate.
$X_{\alpha,\beta,\gamma}$	Variables in α-β-γ coordinate.
$\vec{n}_k$	Normal vector of k-phase.
R_k	Rotation coordinate transformation matrix of k-phase.
P_{adj}	Phase adjustment matrix.
$\vec{V}_{ref}$	Reference voltage vector given in the proposed coordinate transformation.
$V^*_{\alpha s}$, $V^*_{\beta s}$	Reference stationary components given in the proposed coordinate transformation.

The associate editor coordinating the review of this manuscript and approving it for publication was Sudhakar Babu Thanikanti.

I. INTRODUCTION

Presently, owing to the acceleration of problems such as depletion of fossils fuels and environmental pollution, the conventional power grid system is facing an era of change. This change necessitates sustainable power generation using eco-friendly sources such as solar, hydro, wind, and hydrogen fuels [1]. To connect these renewable energy sources to the distribution network, it is necessary to solve various technical problems. Accordingly, the concept of the

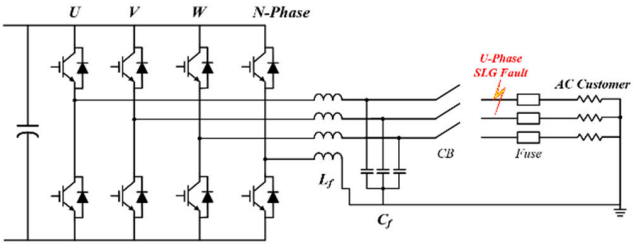

FIGURE 1. Topology of four-leg VSI under SLG fault condition.

microgrid was defined as a solution for the stable integration of distributed generators [2], [3]. A microgrid is a small electrical distribution system that is composed of a power converter, distributed generators, load, and an energy storage system.

Since the introduction of microgrids, a wide range of research into their operation had been conducted, whereas their energy efficiency and power quality have improved along with renewable energy sources. The high power quality of four-leg inverters, in particular, has led to an increasing interest in four-leg microgrids [4], [5].

Principally, several studies have been performed on compensation methods that mitigate the presence of numerous non-linear and unbalanced loads that can occur in four-leg microgrids. [6], [7] proposed the control scheme using a symmetrical sequence decomposition to handle the unbalanced load condition. These functions can provide good power quality to the loads under severe unbalanced conditions. However, faults such as an SLG were not considered in these approaches.

Meanwhile, considerable research has been conducted on fault protection, which is a technique for fault tolerance control based on the power converter topology. However, these studies mainly address the problem of open and short-circuit failures of the semiconductor switch [8], [9]. Therefore, when a failure occurs in a protected distribution area, a blocking and isolation strategy is required to minimize the area affected by the fault.

In [10], [11], additional protection facilities are added in the distribution network to safely separate the fault point when a single line-to-ground (SLG) occurs in power grid. In this case, the load current is cut off through a load-break switch or the fault current is limited by circuit breakers. Additionally, using an automatic circuit recloser, auto shutoff and reclose operations are repeatedly performed to protect the power equipment. Further, various protection coordination operations are performed, these include preventing a failure from spreading through a distribution line by isolating the accident point using a line fuse [12], [13].

However, in the case of simply ensuring the separation from the fault as described above, a problem may occur, preventing power from reaching the other normal loads. If a critical load is connected to the distribution network, significant economic loss can be caused in the event of a power outage owing to an accident.

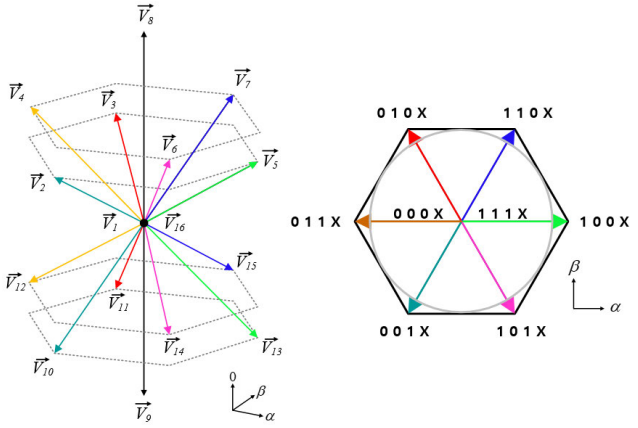

FIGURE 2. Three-phase four-leg VSI output voltage vector (a) 3-D space representation (b) Projection in $\alpha\beta$ plane.

In order to address these problems, the single-phase uninterruptable power supply (UPS) systems where the battery device is connected are widely used as a method of supplying power to the distribution network in case of an accident. However, even when using single-phase UPS systems, certain facilities and control methods are required individually for critical loads [14]. To solve this problem, studies proposing protection coordination logic to locally separate only the fault point using several connectors have been conducted, these approaches include the accurate prediction and detection of the failure point on the power line and the decentralization of the distribution network as much as possible. However, these systems increase the complexity of the power grid and are not suitable for small-scale distribution networks because of the economic burden that comes with the installation of numerous blocking circuits [15]–[19].

In conclusion, the limitation of conventional studies on distribution network fault are as follows: 1) it is necessary to add external equipment to isolate the fault point. 2) It can block up the the normal phases. 3) It increases the complexity of the distribution system. Given the aforementioned reasons, in this paper, we propose fault current isolation using a novel switching method of the four-leg VSI, different from the physical blocking system such as conventional protection circuits. As shown in Fig. 1, when an SLG fault occurs, the use of circuit breakers means power is cut off from the AC load customer. However, the proposed novel switching method applies zero voltage control only on the failed phase. Through this method, power can be continuously supplied to all the other healthy phases with no additional equipment to improve the reliability of islanded microgrid under SLG fault.

The remainder of this paper is organized as follows. Section 2 describes the conventional three-phase four-leg topology, Section 3 details the proposed coordinate transformation method under SLG fault, and Section 4 presents the proposed space vector pulse-width modulation (SVPWM) method. Section 5 and 6 detail the experimental results and conclusions, respectively.

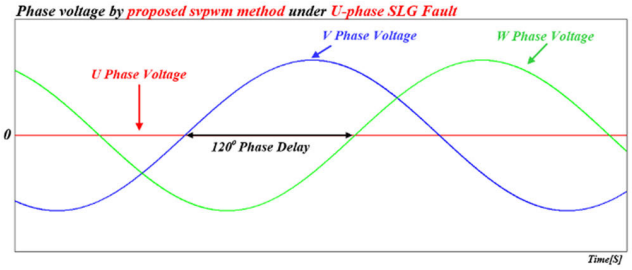

FIGURE 3. Three-phase voltages under U-phase SLG fault by proposed switching method.

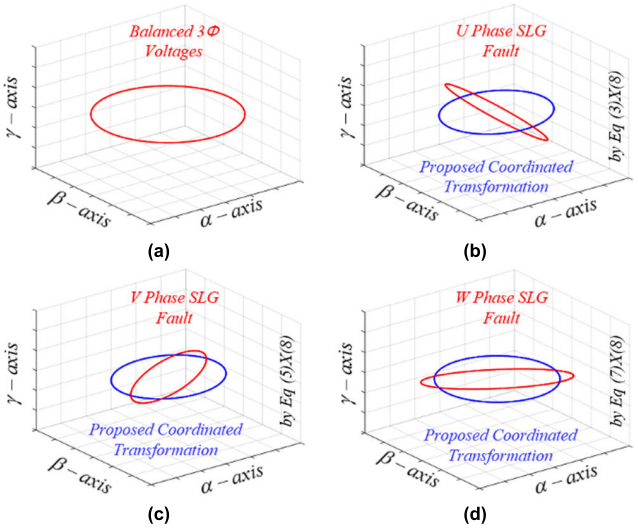

FIGURE 4. Voltage vector trajectories (a) Balanced three phase voltages case (b) U-phase SLG fault case (c) V-Phase SLG fault case (d) W Phase SLG fault case.

II. THREE-PHASE FOUR-LEG INVERTER TOPOLOGY

A three-phase four-leg VSI is shown in Fig. 1. It comprises eight switches at the top and bottom and is divided into fourteen effective voltage vectors and two zero voltage vectors based on the on and off state of the switch. Table 1 summarizes all possible switching vectors and α, β, γ voltages. Fig. 2 expresses the combination of all vectors in space. Particularly, Fig. 2(a) shows a 3-D representation of the four-leg VSI output voltage vector, and Fig. 2(b) shows their projection to the $\alpha\beta$ plane. Unlike the conventional three-leg topology, four-leg VSIs have the advantage of being capable of controlling the zero sequence component during voltage synthesis and can independently control voltages in each phase [20].

Therefore, when an SLG fault occurs, by appropriately selecting and combining voltage vectors, it is possible to control the voltage as shown in Fig. 3. However, before the application of the switching method for voltage control as aforedescribed, a novel coordinate transformation method is required that can detect and control the magnitude of the unbalance three-phase voltage under an SLG fault.

TABLE 1. Normalized four-leg VSI outputs voltages.

	$S_1\,S_2\,S_3\,S_4$	V_{an}	V_{bn}	V_{cn}	V_α	V_β	V_γ
$\vec{V}_1$	0000	0	0	0	0	0	0
$\vec{V}_2$	0010	0	0	1	$-\sqrt{\frac{1}{6}}$	$-\sqrt{\frac{1}{2}}$	$\frac{1}{\sqrt{3}}$
$\vec{V}_3$	0100	0	1	0	$-\sqrt{\frac{1}{6}}$	$\sqrt{\frac{1}{2}}$	$\frac{1}{\sqrt{3}}$
$\vec{V}_4$	0110	0	1	1	$-\sqrt{\frac{2}{3}}$	0	$\frac{2}{\sqrt{3}}$
$\vec{V}_5$	1000	1	0	0	$\sqrt{\frac{2}{3}}$	0	$\frac{1}{\sqrt{3}}$
$\vec{V}_6$	1010	1	0	1	$\sqrt{\frac{1}{6}}$	$-\sqrt{\frac{1}{2}}$	$\frac{2}{\sqrt{3}}$
$\vec{V}_7$	1100	1	1	0	$\sqrt{\frac{1}{6}}$	$\sqrt{\frac{1}{2}}$	$\frac{2}{\sqrt{3}}$
$\vec{V}_8$	1110	1	1	1	0	0	$\sqrt{3}$
$\vec{V}_9$	0001	-1	-1	-1	0	0	$-\sqrt{3}$
$\vec{V}_{10}$	0011	-1	-1	0	$-\sqrt{\frac{1}{6}}$	$-\sqrt{\frac{1}{2}}$	$-\frac{2}{\sqrt{3}}$
$\vec{V}_{11}$	0101	-1	0	-1	$-\sqrt{\frac{1}{6}}$	$\sqrt{\frac{1}{2}}$	$-\frac{2}{\sqrt{3}}$
$\vec{V}_{12}$	0111	-1	0	0	$-\sqrt{\frac{2}{3}}$	0	$-\frac{1}{\sqrt{3}}$
$\vec{V}_{13}$	1001	0	-1	-1	$\sqrt{\frac{2}{3}}$	0	$-\frac{2}{\sqrt{3}}$
$\vec{V}_{14}$	1011	0	-1	0	$\sqrt{\frac{1}{6}}$	$-\sqrt{\frac{1}{2}}$	$-\frac{1}{\sqrt{3}}$
$\vec{V}_{15}$	1101	0	0	-1	$\sqrt{\frac{1}{6}}$	$\sqrt{\frac{1}{2}}$	$-\frac{1}{\sqrt{3}}$
$\vec{V}_{16}$	1111	0	0	0	0	0	0

III. PROPOSED COORDINATE TRANSFORMATION METHOD FOR SLG FAULT CONDITION

As mentioned above, the application of zero voltage to the faulty phase and the supply of normal voltage to the healthy phases under SLG fault conditions is the core of the proposed method. However, when an SLG fault occurs, the desired controlled three-phase voltage to be output is in an unbalanced state; thus, the zero sequence component represented by the γ-axis of the conventional $\alpha\beta\gamma$ plane cannot be zero when using conventional Clarke transformation as shown in (1) [21]. Figure 4 shows the voltage trajectories that appear when the three-phase voltages are in a balanced state and when an SLG fault occurs for each phase, respectively, using the MATLAB tool. As seen in Fig. 4, owing to the γ-axis component, each distorted voltage vector in the form of an ellipse appears as a trajectory rotating in a 3-D plane.

Therefore, because it is impossible to convert a physical quantity of three phases into an AC quantity of two phases

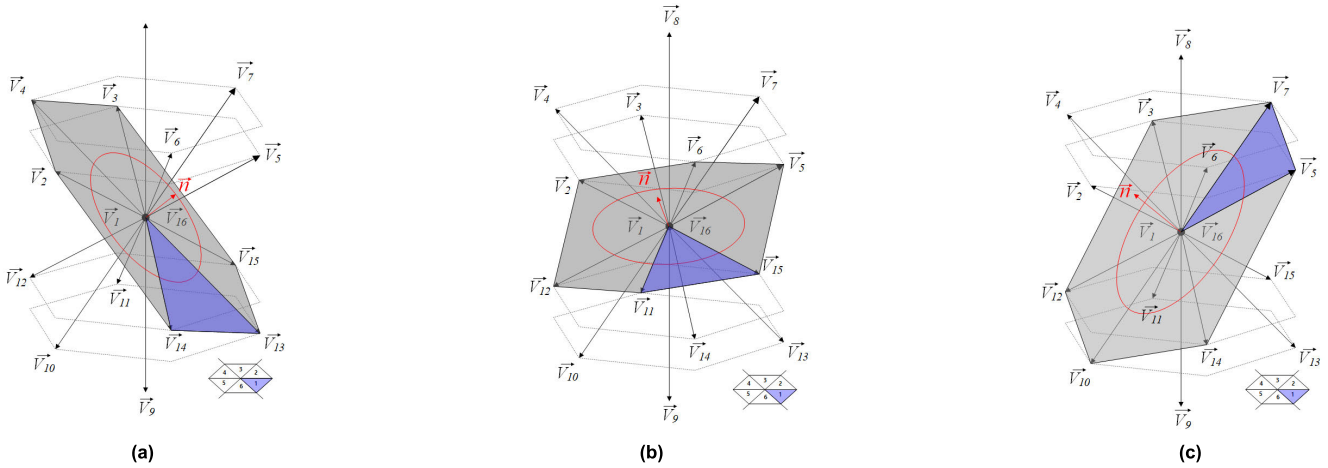

FIGURE 5. 3-D space representation of the four-leg VSI outputs under SLG fault condition (a) u-phase fault case (b) v-phase fault case (c) w-phase fault case.

using (1), it is inevitably difficult to configure the PI voltage controller. To solve this problem, a novel coordinate transformation is required to make the γ-axis component zero and to represent the distorted voltage plane in a new coordinate system. Figure 6 clarifies how the proposed coordinate transformation is applied to the conventional PI controller. If an SLG fault does not occur, the controller is configured using the conventional transformation matrix by (1). However, when an SLG fault occurs, new transformation matrices and a phase adjustment matrix for each phase must be applied. After obtaining the stationary components by the proposed method, the SRF transformation enables the detection and control of the voltage magnitude even under an SLG fault.

In this section, the proposed transformation matrices for rotation in a new coordinate system are obtained using a γ-axis transformation.

$$\begin{bmatrix} X_\alpha \\ X_\beta \\ X_\gamma \end{bmatrix} = \frac{2}{3}\begin{bmatrix} 1 & -1/2 & -1/2 \\ 0 & \sqrt{3}/2 & -\sqrt{3}/2 \\ 1/\sqrt{2} & 1/\sqrt{2} & 1/\sqrt{2} \end{bmatrix} \cdot \begin{bmatrix} X_a \\ X_b \\ X_c \end{bmatrix} \quad (1)$$

A. U-PHASE SLG FAULT

The switching vector for applying the zero voltage to the faulty phase is to make the switching state of that phase and the n-phase the same. Through this principle, the switching vector combination for the application of the proposed method under u-phase SLG fault is selected as follows:

Switching vectors: $\vec{V}_1, \vec{V}_2, \vec{V}_3, \vec{V}_4, \vec{V}_{13}, \vec{V}_{14}, \vec{V}_{15}, \vec{V}_{16}$.

When the selected vectors are connected and displayed as above, it can be observed that the distorted voltage vectors appear based on the combination of specific voltage vectors as shown in Fig. 5. By setting a new γ-axis that exist on this plane and rotating it based on that axis, the proposed coordinate transformation to a new plane is complete. In a scenario where a u-phase fault occurs, the normal vector

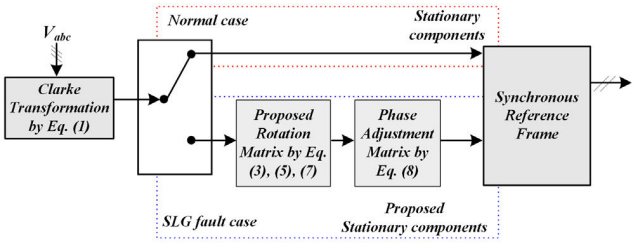

FIGURE 6. Process of proposed coordinate transformation.

$\vec{N}_U$ is obtained from the vector product of $\vec{V}_{14}$ and $\vec{V}_{13}$, as shown in (2). This normal vector, $\vec{N}_U$ obtained in this process becomes the new γ-axis when a u-phase SLG fault occurs. Additionally, it was confirmed that the scalar product of $\vec{N}_U$ and $\vec{V}_{15}$ is zero, meaning six effective vectors and two zero vectors exist on the same plane. After settling the $\vec{N}_U$ obtained through the process above to the new γ-axis, the new α-β axes can be calculated using the relationship between $\vec{V}_{14}$ and $\vec{V}_{13}$. Therefore, when a u-phase SLG fault occurs, the new coordinate transformation matrix $\vec{R}_U$ is obtained as in (3).

$$\begin{aligned} \vec{n}_U &= \vec{V}_{14} \times \vec{V}_{13} \\ &= (1/\sqrt{6}, -1/\sqrt{2}, -1/\sqrt{3}) \times (\sqrt{2}/\sqrt{3}, 0, -2/\sqrt{3}) \\ &= (\sqrt{2}/\sqrt{3}, 0, 1/\sqrt{3}) \end{aligned} \quad (2)$$

$$R_U = \begin{bmatrix} \vec{V}_{14} \\ \vec{V}_{14} \times \vec{V}_{13} \times \vec{V}_{14} \\ \vec{V}_{14} \times \vec{V}_{13} \end{bmatrix} = \begin{bmatrix} 1/\sqrt{6} & -1/\sqrt{2} & -1/3 \\ 1/\sqrt{6} & 1/\sqrt{2} & -1/\sqrt{3} \\ \sqrt{2}/\sqrt{3} & 0 & 1/\sqrt{3} \end{bmatrix} \quad (3)$$

B. V, W-PHASE SLG FAULT

Next, when an SLG fault occurs in the v or w-phases, vectors with the same n-phase switching state are selected and these are shown below:

Switching vectors:$\vec{V}_1, \vec{V}_2, \vec{V}_5, \vec{V}_6, \vec{V}_{11}, \vec{V}_{12}, \vec{V}_{15}, \vec{V}_{16}$
(v-phase)

Switching vectors: $\vec{V}_1, \vec{V}_3, \vec{V}_5, \vec{V}_7, \vec{V}_{10}, \vec{V}_{12}, \vec{V}_{14}, \vec{V}_{16}$

(w-phase)

In the case of a v-phase SLG fault, the vector product of $\vec{V}_5$ and $\vec{V}_6$ is calculated to obtain the normal vector $\vec{N}_V$ through the same principle. Moreover, it was confirmed that all vectors exist on the same plane through the scalar product of $\vec{N}_V$ and $\vec{V}_2$. Using the above method, the transformation matrix under a v-phase fault is obtained as follows.

$$\begin{aligned}\vec{n}_V &= \vec{V}_5 \times \vec{V}_6 \\ &= (\sqrt{2}/\sqrt{3}, 0, 1/\sqrt{3}) \times (1/\sqrt{6}, -1/\sqrt{2}, 2/\sqrt{3}) \\ &= (-1/\sqrt{6}, -\sqrt{2}/2, -1/\sqrt{3}) \end{aligned} \tag{4}$$

$$R_V = \begin{bmatrix} \vec{V}_5 \\ \vec{V}_5 \times \vec{V}_6 \times \vec{V}_5 \\ \vec{V}_5 \times \vec{V}_6 \end{bmatrix} = \begin{bmatrix} \sqrt{2}/\sqrt{3} & 0 & 1/\sqrt{3} \\ -1/\sqrt{6} & -1/\sqrt{2} & 1/\sqrt{3} \\ 1/\sqrt{6} & -\sqrt{2}/2 & -1/\sqrt{3} \end{bmatrix} \tag{5}$$

In the case of a w-phase SLG fault, a new γ-axis can be obtained using the same method. This part is similar to the other cases, thus it is not explained in detail; however, the relevant equations are shown below.

$$\begin{aligned}\vec{n}_W &= \vec{V}_5 \times \vec{V}_7 \\ &= (\sqrt{2}/\sqrt{3}, 0, 1/\sqrt{3}) \times (1/\sqrt{6}, 1/\sqrt{2}, 2/\sqrt{3}) \\ &= (-1/\sqrt{6}, -1/\sqrt{2}, 1/\sqrt{3}) \end{aligned} \tag{6}$$

$$R_W = \begin{bmatrix} \vec{V}_5 \\ \vec{V}_5 \times \vec{V}_7 \times \vec{V}_5 \\ \vec{V}_5 \times \vec{V}_7 \end{bmatrix} = \begin{bmatrix} \sqrt{2}/\sqrt{3} & 0 & 1/\sqrt{3} \\ -1/\sqrt{6} & 1/\sqrt{2} & 1/\sqrt{3} \\ -1/\sqrt{6} & -1/\sqrt{2} & 1/\sqrt{3} \end{bmatrix} \tag{7}$$

In conclusion, the transformation matrices to rotate to a new coordinate plane through the relation of vectors was performed after setting a new γ-axis for SLG faults in each phase. However, the coordinate components transformed through these equations have a phase difference of 120°. Therefore, by applying the phase adjustment matrix as shown in (8), the novel coordinated system has a phase difference of 90°. Consequently, the distortion component for each phase, shown in Fig. 4, is converted into a stationary coordinate component. This component is later used in the configuration of the PI voltage controller through an SRF transformation.

$$P_{adj} = (2/\sqrt{3}) \begin{bmatrix} \sqrt{3}/2 & 0 & 0 \\ 1/2 & 1 & 0 \\ 0 & 0 & \sqrt{3}/2 \end{bmatrix} \tag{8}$$

IV. PROPOSED SVPWM CONTROL STRATEGY

Unlike the proposed coordinate transformation method, it is worth noting that the hexagon where the proposed SVPWM method is actually performed is a distorted plane. Further, to apply this control method under SLG fault conditions in a four-leg inverter, some extra steps are required.

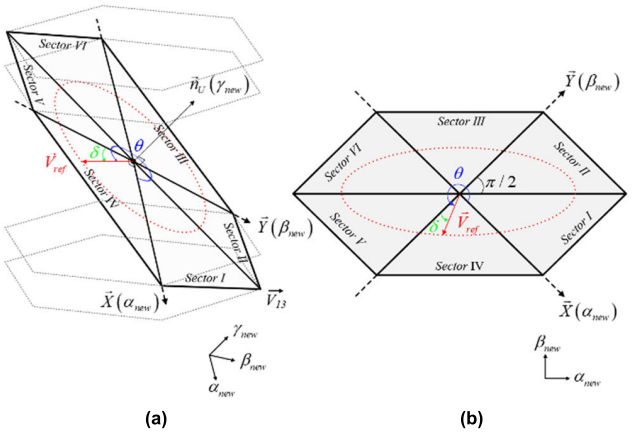

FIGURE 7. Three-phase four-leg VSI output voltage vector under u-phase SLG fault by proposed method (a) 3-D space representation, (b) Projection in $\alpha\beta$ plane.

First, the identification of the reference vector position is needed in the distorted plane owing to the vector selected for a specific situation. Second, the determination of the application intervals and the process of reference vector synthesis are required. Third, building a vector sequence is necessary. A detailed description of this process is provided in this section.

A. SECTOR IDENTIFICATION

To determine the reference vector position, the conventional three-phase four-leg inverter has twenty-four tetrahedrons; however, the proposed scheme controls the switching of a specific phase and the n-phase equally when selecting a switching vector for zero voltage control.

Therefore, the voltage vector diagram is divided into six sectors within the hexagon similar to the 2-D SVPWM method. However, owing to the specific vector selection, this sector identification process has to be operated within a distorted hexagon. Fig. 7 shows the results of projecting a distorted 3-D plane into 2-D after setting a new γ-axis through the proposed coordinate transformation method described above. Here, the X and Y axes represent the reference values of the stationary components in the conventional 2-D SVPWM method. However, because it has a distorted hexagon, all the inner angles are not the same; thus, the size of the sectors appears different. Accordingly, a different calculation process is required to synthesize the reference voltage vector for each sector. In this study, the reference vector position was determined using (9).

$$\begin{aligned} X \geq 0 &\begin{cases} X \geq 0 & \begin{cases} |Y| \leq |X| & (\text{sector} = 1) \\ |Y| > |X| & (\text{sector} = 2) \end{cases} \\ X < 0 & (\text{sector} = 3) \end{cases} \\ Y < 0 &\begin{cases} X < 0 & \begin{cases} |Y| \leq |X| & (\text{sector} = 4) \\ |Y| > |X| & (\text{sector} = 5) \end{cases} \\ X > 0 & (\text{sector} = 6) \end{cases} \end{aligned} \tag{9}$$

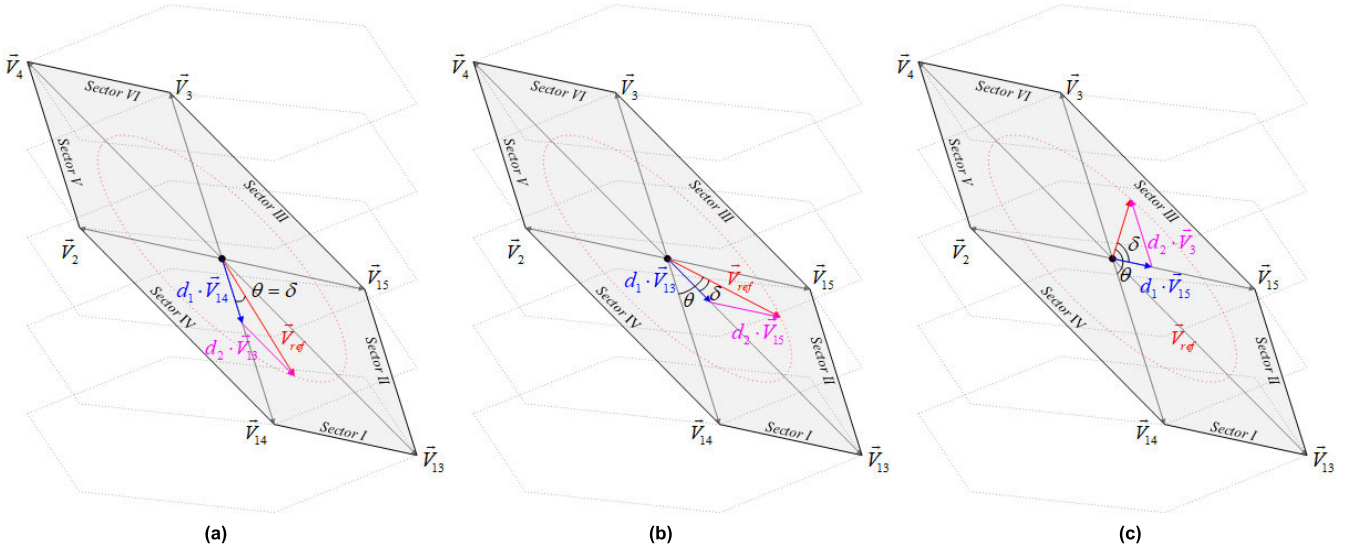

FIGURE 8. 3-D space representation and reference voltage synthesis under u-phase SLG fault case (a) sector I (b) sector II, (c) sector III.

B. DETERMINATION OF THE APPLICATION INTERVALS AND REFERENCE VECTOR SYNTHESIS

When an SLG fault occurs, six voltage vectors can be output using the space vectors of each phase. Therefore, six sectors are given and the method for finding their areas is outlined above. This section describes the process for tracking the reference voltage according to the range of the sector area. For brevity and owing to the symmetry between sectors, not all processes are explained herein. We consider only the reference voltage synthesis process for sectors I, II, and III when a u-phase fault occurs. For example, sector I can be expressed as shown in Fig. 8(a).

Generally, when performing the PWM technique, the output voltage decreases on average and is placed at a point between $\vec{V}_{14}$ and $\vec{V}_{13}$ inside the hexagon. At this point, an arbitrary output voltage vector $\vec{V}_{ref}$ existing between the two vectors is the result of the values obtained from the temporal synthesis that use voltage vectors corresponding to two sides of the triangle that exist at its location. Here, by calculating the coordinates of the voltage vector, the duty ratios d_1, d_2 and $d_0(=1-d_1-d_2)$ can be obtained for reference voltage tracking.

$$\begin{aligned} \vec{V}_{ref} &= d_1\vec{V}_{14} + d_2\vec{V}_{13} \qquad (10)\\ d_1 &= \left|\vec{V}_{ref} \Big/ \vec{V}_{14}\right| [\cos(\delta) - \sin(\delta)]\\ d_2 &= \left|\sqrt{2}\vec{V}_{ref} \Big/ \vec{V}_{13}\right| \sin(\delta) \qquad (11) \end{aligned}$$

where θ and δ refer to the rotation angle around the α-axis and the rotation angle in each section, respectively. Next, Fig. 8(b) shows the reference voltage synthesis process for sector II. Similarly, an arbitrary output voltage vector $\vec{V}_{ref}$ between $\vec{V}_{13}$ and $\vec{V}_{15}$, and the duty ratios were obtained as follows.

$$\vec{V}_{ref} = d_1\vec{V}_{13} + d_2\vec{V}_{15} \qquad (12)$$

$$\begin{aligned} d_1 &= \left|\vec{V}_{ref} \Big/ \vec{V}_{13}\right| [\cos(\delta) - \sin(\delta)]\\ d_2 &= \left|\sqrt{2}\vec{V}_{ref} \Big/ \vec{V}_{15}\right| \sin(\delta) \qquad (13) \end{aligned}$$

In the case of sector III, it can be described as follows.

$$\vec{V}_{ref} = d_1\vec{V}_{15} + d_2\vec{V}_{3} \qquad (14)$$

$$\begin{aligned} d_1 &= \left|\vec{V}_{ref} \Big/ \vec{V}_{3}\right| \cos(\delta)\\ d_2 &= \left|\vec{V}_{ref} \Big/ \vec{V}_{12}\right| \sin(\delta) \qquad (15) \end{aligned}$$

The calculation process for duty ratios mentioned above includes the reference voltage, the rotation angle conversion for each sector, and the trigonometric function calculations. Therefore, finally, the rotation angle from the α-axis is converted through the proposed SVPWM voltage vector diagram. Based on this process, it is necessary to analyze the process of calculating the switching application time for each sector. Table 2 summarizes the rotation angle conversion for each sector. For this process, the position of the sector for each phase was selected as shown in Fig. 5. Because the proposed SVPWM voltage vector diagram appears as a distorted hexagon, it is apparent that it has a different conversion value from the conventional 2-D SVPWM method.

After performing the angle conversion using Table 2, the duty ratio for each sector is generalized as follows. The detailed calculation processes for each sector are left in the the appendix A.

$$\begin{cases} d_1 = \dfrac{1}{|\vec{V}_A|}\left[\begin{array}{l} V^*_{\alpha s}(\cos(n\pi) + \sin(n\pi)) \\ \qquad + V^*_{\beta s}(\sin(n\pi) - \cos(n\pi)) \end{array}\right] \\ d_2 = \dfrac{\sqrt{2}}{|\vec{V}_B|}\left[V^*_{\beta s}\cos(n\pi) - V^*_{\alpha s}\sin(n\pi)\right] \\ (if\ \text{sector} = 1, 2, 4, 5) \end{cases} \qquad (16)$$

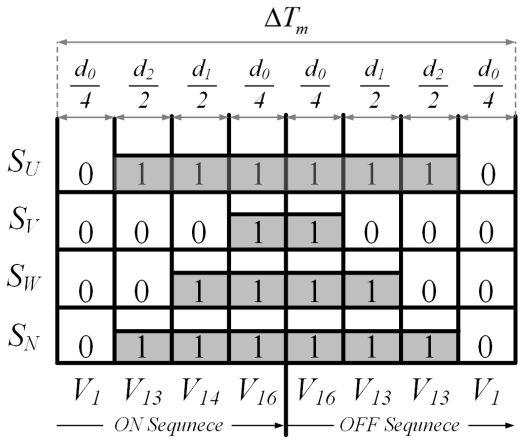

FIGURE 9. Symmetrically aligned modulation scheme.

TABLE 2. Rotation angle conversion for each sector.

SECTOR	δ	n
I	θ	0
II	$\theta-\pi/4$	1/4
III	$\theta-\pi/2$	1/2
IV	$\theta-\pi$	1
V	$\theta-5\pi/4$	5/4
VI	$\theta-6\pi/4$	6/4

$$\begin{cases} d_1 = \frac{1}{|\vec{V}_A|}\left[V^*_{\alpha s}\cos(n\pi) + V^*_{\beta s}\sin(n\pi)\right] \\ d_2 = \frac{1}{|\vec{V}_B|}\left[V^*_{\beta s}\cos(n\pi) - V^*_{\alpha s}\sin(n\pi)\right] \\ (if\ \text{sector} = 3, 6) \end{cases} \tag{17}$$

where $\vec{V}_A$ and $\vec{V}_B$ denote two effective vectors that exist in the sector, and $V^*_{\alpha s}$ and $V^*_{\beta s}$ refer to stationary components that are the reference values of the proposed coordinate transformation. n represents the substitution value for each sector for the generalization of the equations.

C. BULDING A VECTOR SEQUENCE

The process of obtaining the reference voltage and duty ratio for each sector is described in preceding sections. By synthesizing the selected six effective vectors and two zero vectors within the modulation period, the average value of the output voltage can be obtained the same regardless of the vector arrangement. However, in this study, the symmetrically aligned modulation scheme, which is generally known to give superior performance in harmonic, was used [22].

To achieve this, the method shown in Fig. 8 is applied such that the effective voltage vector always exists in the center within a modulation period. Here, when an SLG fault occurs for each phase, the process of how to position these eight vectors can be indicated. Moreover, to calculate the duty ratio of the switching vector, it is necessary to calculate the switching function in all sectors for each phase. As the explanation of this part includes a lot of mundane details, information on the sequence and calculation of duty ratios is included in an appendix B.

TABLE 3. Parameters of simulation and experiment.

Parameter	Value	Unit
DC input voltage	380	*Vdc*
Capacitance (C_f)	22	*μF*
Converter Side Inductance (L_c)	1.5	*mH*
AC Output Voltage (line to line)	190	*V_{rms}*
AC Load (per phase)	900	*W*
Switching frequency (f_s)	10	*kHz*
Power switch (CAS120M12BM2)	-	-

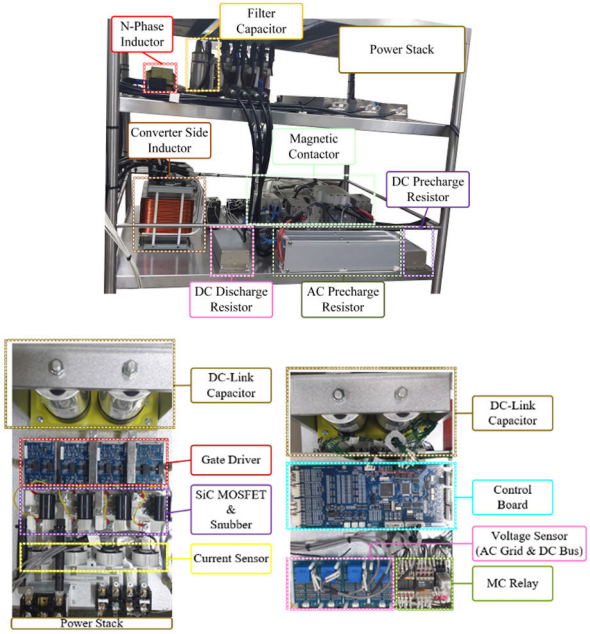

FIGURE 10. Hardware configuration of three-phase four-leg inverter system for experiments.

V. VERIFICATION OF THE PROPOSED METHOD

To verify the feasibility and effectiveness of the proposed method, some experiments and simulations were conducted. The hardware configuration and parameters of the three-phase four-leg inverter system used in the experiment are shown in Fig. 10 and Table 3. In the experiment, the coordinate transformation and the SVPWM method under SLG fault

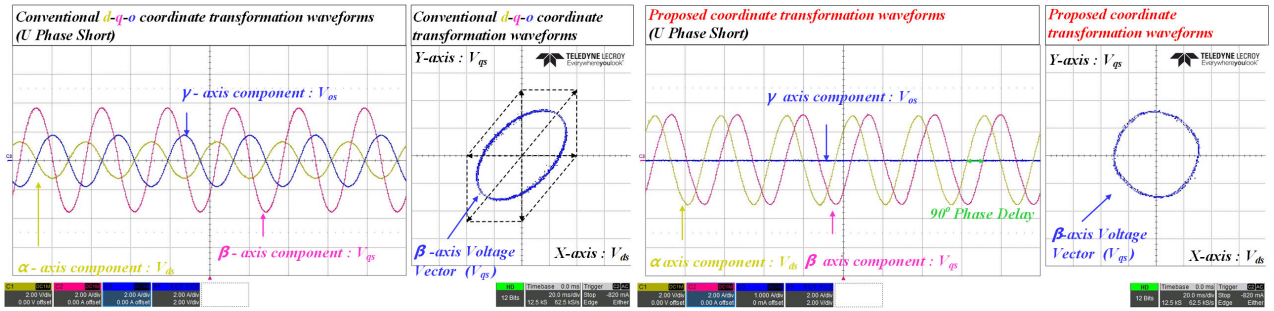

FIGURE 11. U-phase fault condition experiment results (a) conventional coordinate transformation, (b) proposed coordinate transformation.

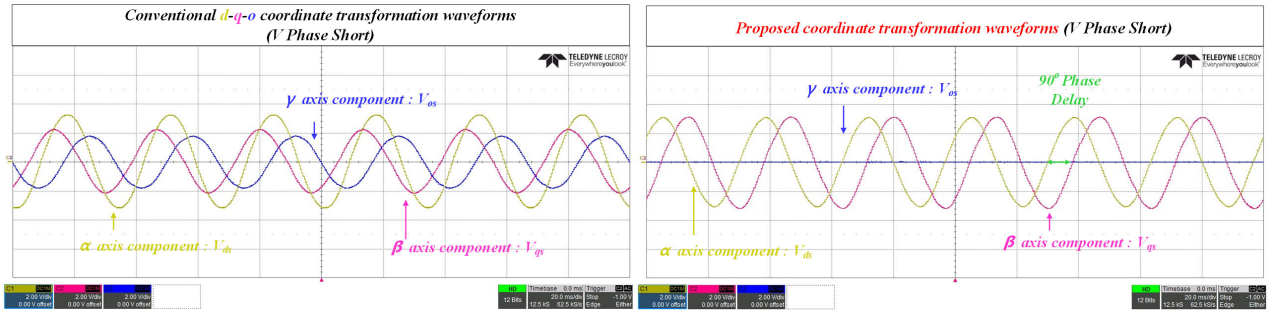

FIGURE 12. V-phase fault condition experiment results (a) conventional coordinate transformation, (b) proposed coordinate transformation.

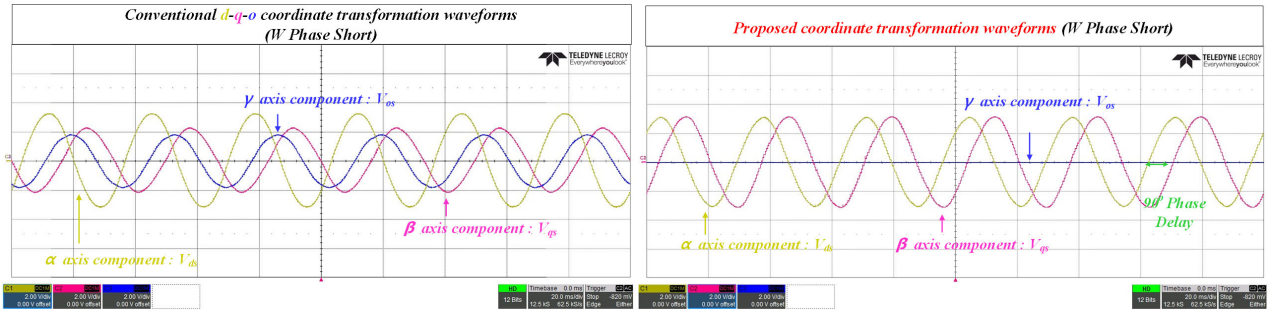

FIGURE 13. W-phase fault condition experiment results (a) conventional coordinate transformation, (b) proposed coordinate transformation.

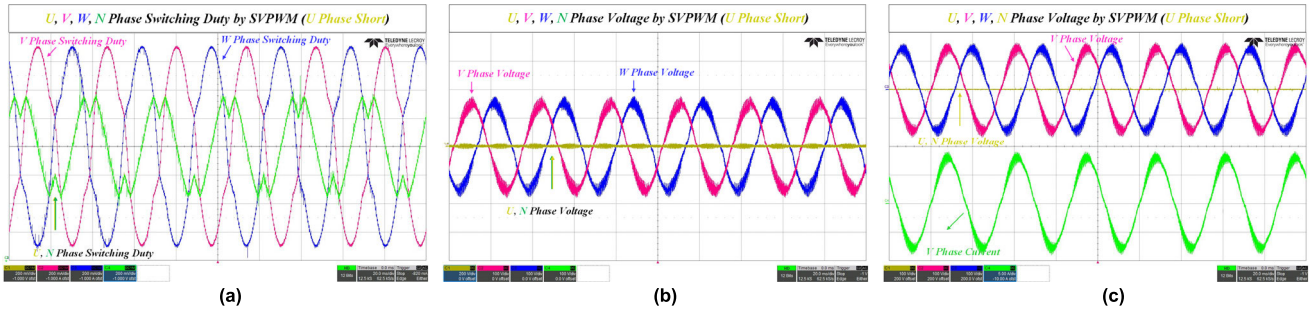

FIGURE 14. Waveforms of the proposed SVPWM method under u-phase SLG fault condition (a) switching duty, (b) output voltages (c) output voltages and current.

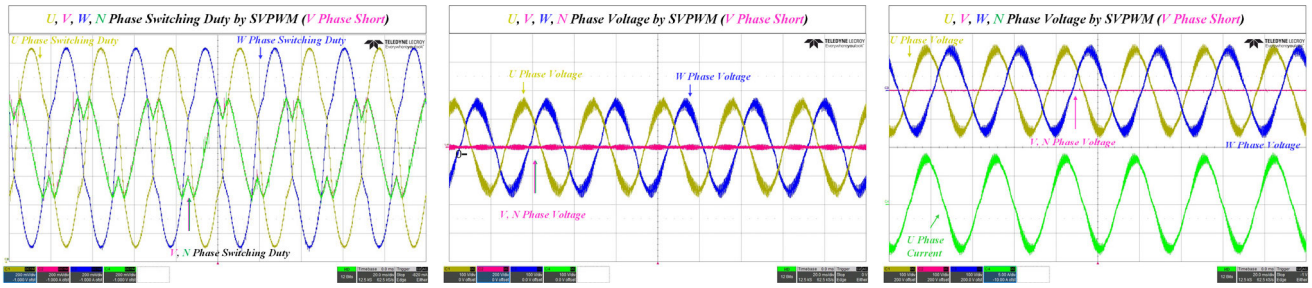

FIGURE 15. Waveforms of the proposed SVPWM method under v-phase SLG fault condition (a) switching duty, (b) output voltages (c) output voltages and current.

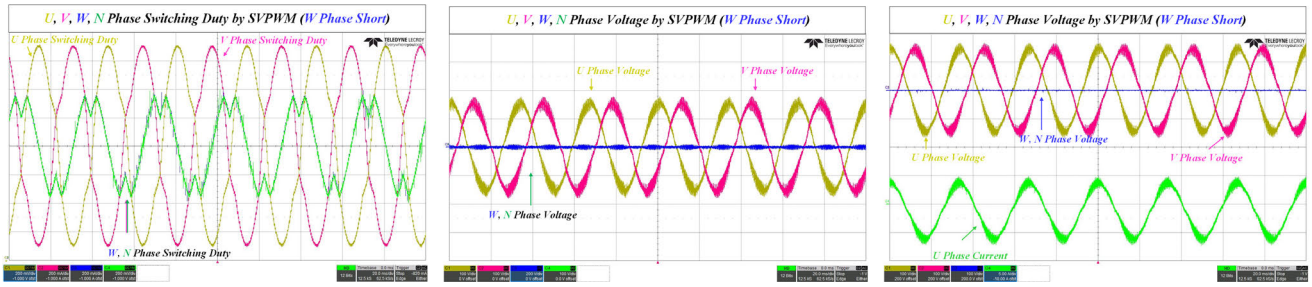

FIGURE 16. Waveforms of the proposed SVPWM method under w-phase SLG fault condition (a) switching duty, (b) output voltages (c) output voltages and current.

conditions were applied. And the efficiency and loss of the inverter system was analyzed through the PSIM simulation. In simulation circuit, the thermal module of the power switch (CAS120M12BM2) was used. The parasitic components of the filter were also considered.

A. PROPOSED COORDINATE TRANSFORMATION

Figs. 11-13 show the experimental waveforms from the coordinate transformation method for each phase. Notably, the voltage to be transformed or observed through the proposed method is the output voltage of three phases, that is, the unbalanced voltage output through the proposed SVPWM method in case of SLG fault. Fig. 11(a) shows the waveforms given by a conventional stationary coordinate transformation when the u-phase voltage is controlled to zero owing to an SLG fault on the u-phase. As seen in the X-Y plot, the stationary components have a distorted trajectory. Fig. 11(b) confirms that the complete stationary components can be obtained through the proposed coordinate transformation. Additionally, it is shown through the X-Y plot that it has the trajectory of the normal voltage vector. Further, Fig. 12(a) and Fig. 13(a) show the waveforms of the conventional method in the case of an SLG fault on the v and w-phases, respectively. Because the waveforms are distorted, it is difficult to accurately detect the magnitude of the voltage. By applying the proposed method, a novel coordinate system can be made as shown in Figs. 12(b) and 13(b), this allows the detection of the voltage level. As mentioned above, the stationary components

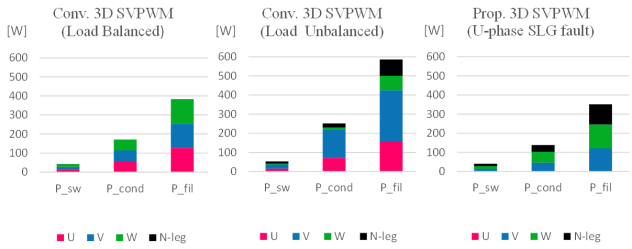

FIGURE 17. Comparison of losses between conventional method and proposed method.

TABLE 4. Comparison of effciencies between conventional method and proposed method.

	Conv. 3D SVPWM (Load Balanced)	Conv. 3D SVPWM (Load Unbalanced)	Prop. 3D SVPWM (U-phase SLG fault)
P_{sw} [w]	42	53	40
P_{cond} [w]	170	252	138
P_{fil} [w]	446	501	288
Efficiency [%]	96.8	96	96.5

obtained through the proposed method are converted to SRF to use as the input to the PI voltage controller in the proposed SVPWM method.

TABLE 5. Switching duty ratio based on sector and each fault case.

Sector	d_1	d_2	*U Phase*		*V Phase*		*W Phase*	
			$\vec{V}_A$	$\vec{V}_B$	$\vec{V}_A$	$\vec{V}_B$	$\vec{V}_A$	$\vec{V}_B$
I	$\frac{1}{\lvert\vec{V}_A\rvert}(V^*_{\alpha s}-V^*_{\beta s})$	$\frac{\sqrt{2}}{\lvert\vec{V}_B\rvert}V^*_{\beta s}$	$\vec{V}_{14}$	$\vec{V}_{13}$	$\vec{V}_5$	$\vec{V}_6$	$\vec{V}_5$	$\vec{V}_7$
II	$\frac{\sqrt{2}}{\lvert\vec{V}_A\rvert}V^*_{\alpha s}$	$\frac{1}{\lvert\vec{V}_B\rvert}(V^*_{\beta s}-V^*_{\alpha s})$	$\vec{V}_{13}$	$\vec{V}_{15}$	$\vec{V}_6$	$\vec{V}_2$	$\vec{V}_7$	$\vec{V}_3$
III	$\frac{1}{\lvert\vec{V}_A\rvert}V^*_{\beta s}$	$-\frac{1}{\lvert\vec{V}_B\rvert}V^*_{\alpha s}$	$\vec{V}_{15}$	$\vec{V}_3$	$\vec{V}_2$	$\vec{V}_{12}$	$\vec{V}_3$	$\vec{V}_{12}$
IV	$\frac{1}{\lvert\vec{V}_A\rvert}(-V^*_{\alpha s}+V^*_{\beta s})$	$-\frac{\sqrt{2}}{\lvert\vec{V}_B\rvert}V^*_{\beta s}$	$\vec{V}_3$	$\vec{V}_4$	$\vec{V}_{12}$	$\vec{V}_{11}$	$\vec{V}_{12}$	$\vec{V}_{10}$
V	$-\frac{\sqrt{2}}{\lvert\vec{V}_A\rvert}V^*_{\alpha s}$	$\frac{1}{\lvert\vec{V}_B\rvert}(-V^*_{\beta s}+V^*_{\alpha s})$	$\vec{V}_4$	$\vec{V}_2$	$\vec{V}_{11}$	$\vec{V}_{15}$	$\vec{V}_{10}$	$\vec{V}_{14}$
VI	$-\frac{1}{\lvert\vec{V}_A\rvert}V^*_{\beta s}$	$\frac{1}{\lvert\vec{V}_B\rvert}V^*_{\alpha s}$	$\vec{V}_2$	$\vec{V}_{14}$	$\vec{V}_{15}$	$\vec{V}_5$	$\vec{V}_{14}$	$\vec{V}_5$

B. PROPOSED SPACE VECTOR PWM METHOD

Fig. 14 shows the waveforms made by applying the proposed method under a u-phase SLG fault. First, when a u-phase fault occurs, the switching duty of all phases is confirmed as shown in Fig. 14(a). As seen in the figure, the faulty u and n-phases have the same switching duty, such that a phase voltage will not be generated because they are in an equipotential state. As shown in Fig. 14(b), the reference of the actual voltage that will appear based on the switching duty shown in this way is verified through the waveforms of the digital-analog converter. Fig. 14(c) shows the waveforms tested in connection with the AC load. When a u-phase fault occurs, zero voltage is applied to the u-phase and normal voltages are applied to the remaining healthy phases. Further, the v-phase current is shown. Moreover, Fig. 15(a) shows the duty when a v-phase fault occurs. It shows that the switching duty of the v and n-phases have the same waveforms. Thus, the same output reference appears as shown in Fig. 15(b). From Fig. 15(c), it is confirmed that zero voltage was supplied to the faulty v-phase. Finally, Fig. 16 shows the experimental waveforms for the w-phase fault. As expected, it confirms that the duty of the w and the n-phases were the same, zero voltage was applied to the w-phase, and the voltage and current were applied only to the loads in the other phases.

C. EFFICIENCY AND LOSS

Fig. 17 shows the comparisons of the inverter losses and filter losses between the conventional 3-D SVPWM method and proposed SVPWM method. P_{sw} *and* P_{cond} denote the switching loss and conduction loss of the power switches, and P_{fil} denotes loss in LC filter. In simulation, the rated load, 20kW class balanced and unbalanced load was used. Under balanced load condition, the loss in the n-leg switches is virtually zero. However, the loss increases as the n-phase current increases under unbalanced load condition. In proposed method, there is no loss in the u-phase switches because a zero voltage is supplied to the u-phase. Table 4 lists the overall efficiencies of the inverter system at the rated 6.6kW per phase.

VI. CONCLUSION

A novel SVPWM control strategy for four-leg inverters under SLG fault in an islanded microgrid is proposed herein. The proposed part is divided into the proposed coordinate transformation method for the detection of unbalanced voltage and a novel SVPWM scheme for driving the four-leg inverter under SLG fault. In the coordinate transformation method, a MATLAB tool was used to analyze the unbalanced voltage trajectories in a new plane. Additionally, a process for setting a new axis through mathematical analysis was presented. Further, a new vector combination for the application of a zero voltage to the faulty phase is proposed in the novel PWM scheme. The implementation of the proposed SVPWM method involves, 1) the process of sector identification in the new plane, 2) synthesis of the voltage reference, and 3) the building of vector sequences are additionally described. The above process was experimentally verified by constructing a 10-kW class three-phase four-leg inverter.

APPENDIX A

The process of calculating the switching duty ratio for the voltage vector synthesis has been described in the previous section IV. Along with the detailed process for obtaining (16) and (17), the duty ratios for each sector using these equations

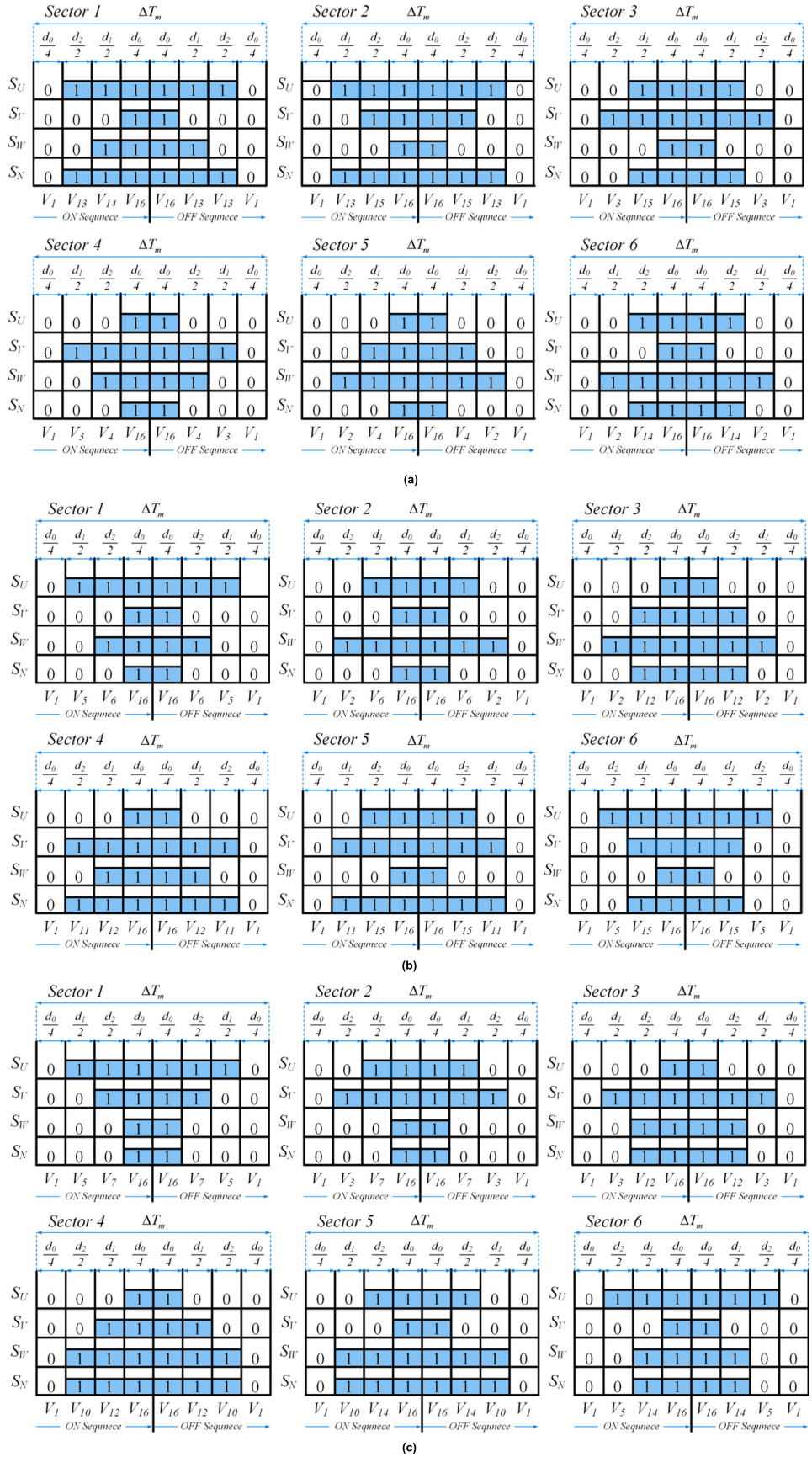

FIGURE 18. Symmetrically aligned modulation scheme applied to the proposed method (a) u-phase fault condition, (b) v-phase fault condition (c) w-phase fault condition.

are shown in Table 5. The proposed SVPWM method has a distorted hexagonal shape different from that of the conventional 2-D SVPWM. For this reason, it can be obtained (16) and (17) by considering internal angle. The detailed explanation is as follows.

First, the case where voltage reference is in sector I, II, IV and V can be obtained by (16). By applying the trigonometric function, (10) and (11) were obtained. These can be given by (A1) and (A2) for the general form.

$$\begin{aligned} \vec{V}_{ref} &= d_1\vec{V}_A + d_2\vec{V}_B \\ &\quad (if\ \text{sector} = 1, 2, 4, 5) \end{aligned} \tag{A1}$$

$$\begin{aligned} d_1 &= \left|\vec{V}_{ref}\middle/\vec{V}_A\right|(\cos\delta - \sin\delta) \\ d_2 &= \left|\sqrt{2}\vec{V}_{ref}\middle/\vec{V}_B\right|\sin\delta \\ &\quad (if\ \text{sector} = 1, 2, 4, 5) \end{aligned} \tag{A2}$$

Next, the process for angle conversion was used by Table 2 (i.e. $\delta = \theta - n\pi$). Therefore, the switching duty ratios can be described by (A3) and (A4).

$$\begin{aligned} d_1 &= \left|\vec{V}_{ref}\middle/\vec{V}_A\right|(\cos\delta - \sin\delta) \\ &= \frac{\left|\vec{V}_{ref}\right|}{\left|\vec{V}_A\right|}[\cos(\theta - n\pi) - \sin(\theta - n\pi)] \\ &= \frac{\left|\vec{V}_{ref}\right|}{\left|\vec{V}_A\right|}\begin{bmatrix}\cos\theta\,(\cos(n\pi) + \sin(n\pi)) \\ \quad + \sin\theta\,(\sin(n\pi) - \cos(n\pi))\end{bmatrix} \\ &= \frac{1}{\left|\vec{V}_A\right|}\begin{bmatrix}V^*_{\alpha s}\,(\cos(n\pi) + \sin(n\pi)) \\ \quad + V^*_{\beta s}\,(\sin(n\pi) - \cos(n\pi))\end{bmatrix} \\ &\quad (if\ \text{sector} = 1, 2, 4, 5) \end{aligned} \tag{A3}$$

$$\begin{aligned} d_2 &= \left|\sqrt{2}\vec{V}_{ref}\middle/\vec{V}_B\right|\sin\delta \\ &= \frac{\left|\vec{V}_{ref}\right|}{\left|\vec{V}_B\right|}\sqrt{2}\cdot\sin(\theta - n\pi) \\ &= \frac{\left|\vec{V}_{ref}\right|}{\left|\vec{V}_B\right|}[\sin\theta\cdot\cos n\pi - \cos\theta\cdot\sin n\pi] \\ &= \frac{\sqrt{2}}{\left|\vec{V}_B\right|}\left[V^*_{\beta s}\cos(n\pi) - V^*_{\alpha s}\sin(n\pi)\right] \\ &\quad (if\ \text{sector} = 1, 2, 4, 5) \end{aligned} \tag{A4}$$

In case that reference voltage is in sector III and VI, duty ratios can be expressed by (17). Through trigonometric calculations, (14) and (15) can be obtained. It can be written as the general form shown in (A5) and (A6).

$$\begin{aligned} \vec{V}_{ref} &= d_1\vec{V}_A + d_2\vec{V}_B \\ &\quad (if\ \text{sector} = 3, 6) \end{aligned} \tag{A5}$$

$$\begin{aligned} d_1 &= \left|\vec{V}_{ref}\middle/\vec{V}_A\right|\cos\delta \\ d_2 &= \left|\vec{V}_{ref}\middle/\vec{V}_B\right|\sin\delta \\ &\quad (if\ \text{sector} = 3, 6) \end{aligned} \tag{A6}$$

By applying the angle conversion, the duty ratios can be given by (A7) and (A8).

$$\begin{aligned} d_1 &= \left|\vec{V}_{ref}\middle/\vec{V}_A\right|\cos\delta \\ &= \left|\vec{V}_{ref}\middle/\vec{V}_A\right|\cos(\theta - n\pi) \\ &= \frac{\left|\vec{V}_{ref}\right|}{\left|\vec{V}_A\right|}[\cos\theta\cdot\cos n\pi + \sin\theta\cdot\sin n\pi] \\ &= \frac{1}{\left|\vec{V}_A\right|}\left[V^*_{\alpha s}\cos(n\pi) + V^*_{\beta s}\sin(n\pi)\right] \\ &\quad (if\ \text{sector} = 3, 6) \end{aligned} \tag{A7}$$

$$\begin{aligned} d_2 &= \left|\vec{V}_{ref}\middle/\vec{V}_B\right|\sin\delta \\ &= \left|\vec{V}_{ref}\right|\sin(\theta - n\pi)\middle/\left|\vec{V}_B\right| \\ &= \frac{\left|\vec{V}_{ref}\right|}{\left|\vec{V}_B\right|}[\sin\theta\cdot\cos n\pi - \cos\theta\cdot\sin n\pi] \\ &= \frac{1}{\left|\vec{V}_B\right|}\left[V^*_{\beta s}\cos(n\pi) - V^*_{\alpha s}\sin(n\pi)\right] \\ &\quad (if\ \text{sector} = 3, 6) \end{aligned} \tag{A8}$$

Through the above process, the generalized equations for the duty ratio for each sector were obtained.

APPENDIX B

The sequence of the symmetrically aligned modulation scheme using the vector combination selected through the proposed switching method is shown in Fig. 18.

REFERENCES

[1] D. P. Silva, J. L. Félix Salles, J. F. Fardin, and M. M. Rocha Pereira, "Management of an island and grid-connected microgrid using hybrid economic model predictive control with weather data," *Appl. Energy*, vol. 278, Nov. 2020, Art. no. 115581.

[2] R. Ramakumar, "Role of distributed generation in reinforcing the critical electric power infrastructure," in *Proc. IEEE Power Eng. Soc. Winter Meeting Conf.*, Feb. 2001, p. 139, doi: 10.1109/PESW.2001.917016.

[3] R. H. Lasseter, "MicroGrids," in *Proc. IEEE Power Eng. Soc. Winter Meeting Conf.*, vol. 1, Jan. 2002, pp. 305–308, doi: 10.1109/PESW.2002.985003.

[4] M. Rivera, V. Yaramasu, A. Llor, J. Rodriguez, B. Wu, and M. Fadel, "Digital predictive current control of a three-phase four-leg inverter," *IEEE Trans. Ind. Electron.*, vol. 60, no. 11, pp. 4903–4912, Nov. 2013, doi: 10.1109/TIE.2012.2219837.

[5] M. R. Miveh, M. F. Rahmat, A. A. Ghadimi, and M. W. Mustafa, "Control techniques for three-phase four-leg voltage source inverters in autonomous microgrids: A review," *Renew. Sustain. Energy Rev.*, vol. 54, pp. 1592–1610, Feb. 2016.

[6] A. Mohd, E. Ortjohann, N. Hamsic, and W. Sinsukthavorn, "Control strategy and space vector modulation for three-leg four-wire voltage source inverters under unbalanced load conditions," *IET Power Electron.*, vol. 3, no. 33, pp. 323–333, 2010.

[7] I. Vechiu, O. Curea, and H. Camblong, "Transient operation of a four-leg inverter for autonomous applications with unbalanced load," *IEEE Trans. Power Electron.*, vol. 25, no. 2, pp. 399–407, Feb. 2010, doi: 10.1109/TPEL.2009.2025275.

[8] Z. Zeng, W. Zheng, R. Zhao, C. Zhu, and Q. Yuan, "The comprehensive design and optimization of the post-fault grid-connected three-phase PWM rectifier," *IEEE Trans. Ind. Electron.*, vol. 63, no. 3, pp. 1629–1642, Mar. 2016, doi: 10.1109/TIE.2015.2494854.

[9] W. S. Im, J. M. Kim, D. C. Lee, and K. B. Lee, "Diagnosis and fault-tolerant control of three-phase AC-DC PWM converter systems," *IEEE Trans. Ind. Appl.*, vol. 49, no. 4, pp. 1539–1547, Jul./Aug. 2013, doi: 10.1109/TIA.2013.2255111.

[10] P. Basak, S. Chowdhury, S. Halder nee Dey, and S. P. Chowdhury, "A literature review on integration of distributed energy resources in the perspective of control, protection and stability of microgrid," *Renew. Sustain. Energy Rev.*, vol. 16, no. 8, pp. 5545–5556, Oct. 2012.

[11] R. Firestone and C. Marnay, "Energy manager design for microgrids," Consortium Electr. Rel. Technol. Solutions, Lawrence Berkeley Nat. Lab., California Energy Commission, Sacramento, CA, USA, Tech. Rep. LBNL-54447, Jan. 2005.

[12] D. M. Bui, S.-L. Chen, C.-H. Wu, K.-Y. Lien, C.-H. Huang, and K.-K. Jen, "Review on protection coordination strategies and development of an effective protection coordination system for DC microgrid," in *Proc. IEEE PES Asia–Pacific Power Energy Eng. Conf. (APPEEC)*, Dec. 2014, pp. 1–10, doi: 10.1109/APPEEC.2014.7066159.

[13] I. Almutairy, "A review of coordination strategies and techniques for overcoming challenges to microgrid protection," in *Proc. Saudi Arabia Smart Grid (SASG)*, Dec. 2016, pp. 1–4, doi: 10.1109/SASG.2016.7849681.

[14] H. Li, M. Chen, B. Yang, F. Blaabjerg, and D. Xu, "Fast fault protection based on direction of fault current for the high-surety power-supply system," *IEEE Trans. Power Electron.*, vol. 34, no. 6, pp. 5787–5802, Jun. 2019, doi: 10.1109/TPEL.2018.2870982.

[15] S. M. Blair, C. D. Booth, G. M. Burt, and C. G. Bright, "Application of multiple resistive superconducting fault-current limiters for fast fault detection in highly interconnected distribution systems," *IEEE Trans. Power Del.*, vol. 28, no. 2, pp. 1120–1127, Apr. 2013, doi: 10.1109/TPWRD.2012.2228011.

[16] F. Zheng, C. Deng, L. Chen, S. Li, Y. Liu, and Y. Liao, "Transient performance improvement of microgrid by a resistive superconducting fault current limiter," *IEEE Trans. Appl. Supercond.*, vol. 25, no. 3, pp. 1–5, Jun. 2015, Art. no. 5602305, doi: 10.1109/TASC.2015.2391120.

[17] K. Moloi and A. A. Yusuff, "Power distribution system fault diagnostic using genetic algorithm and neural network," in *Proc. Southern Afr. Universities Power Eng. Conf./Robot. Mechatronics/Pattern Recognit. Assoc. South Afr. (SAUPEC/RobMech/PRASA)*, Jan. 2021, pp. 1–5, doi: 10.1109/SAUPEC/RobMech/PRASA52254.2021.9377241.

[18] M. A. Barik, A. Gargoom, M. A. Mahmud, M. E. Haque, H. Al-Khalidi, and A. M. T. Oo, "A decentralized fault detection technique for detecting single phase to ground faults in power distribution systems with resonant grounding," *IEEE Trans. Power Del.*, vol. 33, no. 5, pp. 2462–2473, Oct. 2018, doi: 10.1109/TPWRD.2018.2799181.

[19] L. Zamboni, I. Nunes da Silva, L. Nascimento Soares, and R. A. Souza Fernandes, "Fault detection in power distribution systems using automated integration of computational intelligence tools," *IEEE Latin Amer. Trans.*, vol. 9, no. 4, pp. 522–527, Jul. 2011, doi: 10.1109/TLA.2011.5993738.

[20] Q.-C. Zhong, J. Liang, G. Weiss, C. Feng, and T. Green, "H_∞ control of the neutral point in 4-wire 3-phase DC-AC converters," *IEEE Trans. Ind. Electron.*, vol. 53, no. 5, pp. 1594–1602, Nov. 2006.

[21] J. I. Y. Ota, M. G. Villalva, F. Sato, and E. Ruppert, "3-D space vector PWM implementation for four-leg voltage source inverter," in *Proc. XI Brazilian Power Electron. Conf.*, Sep. 2011, pp. 79–86, doi: 10.1109/COBEP.2011.6085206.

[22] R. Zhang, V. H. Prasad, D. Boroyevich, and F. C. Lee, "Three-dimensional space vector modulation for four-leg voltage-source converters," *IEEE Trans. Power Electron.*, vol. 17, no. 3, pp. 314–326, May 2002, doi: 10.1109/TPEL.2002.1004239.